Oscillatory exchange coupling across $Cu_{1-x}Ni_x$ spacers: A first-principles calculation of the amplitudes and phases using asymptotic analysis

N. N. Lathiotakis and B. L. Györffy
H. H. Wills Physics Laboratory, University of Bristol, Tyndall Avenue, BS8 1TL Bristol, United Kingdom

E. Bruno and B. Ginatempo
Dipartimento di Fisica and Unità INFM, Università di Messina, Salita Sperone 31, 98166 Messina, Italy
(Received 5 May 2000)

We apply a recently developed first-principles asymptotic approach to the problem of the oscillatory exchange coupling (OEC) in the $Co/Cu_{(1-x)}Ni_x/Co$ trilayer system for all (100), (110), and (111) directions of growth. We compare results of the asymptotic analysis with full calculations. Our results are consistent with the available experimental data and give strong evidence for the existence of the exponential decay in the asymptotic form of the OEC for $x>0.04$. Moreover, we discover a caliper vector of the alloy Fermi surface $Q^{(3)}_{(100)}$ which did not exist in the case of pure Cu, but contributes to the OEC significantly for $x \geqslant 0.11$.

I. INTRODUCTION

One of the most fascinating aspects of the oscillatory exchange coupling (OEC) of two Ferromagnetic layers across a nonmagnetic metallic spacer layer[1–3] is the connection of the coupling characteristics, i.e., periods, amplitudes, and phases, to the Fermi surface of the bulk spacer material.[4–8] While the related effect of giant magnetoresistance[6] (GMR) has already found its way to the production line, there is still significant scientific interest in the OEC (Refs. 7–13) and that interest is focused on the connection of the effect to the Fermi surface properties. Namely, it appears to be the case that the OEC may be regarded as a major probe of the Fermi surfaces of materials such as the random binary alloys.[8]

More specifically, from the theoretical point of view, it has been proven that the coupling energy of two ferromagnetic layers separated by a paramagnetic one can be decomposed into terms which oscillate as functions of spacer thickness.[4] The wave number of each oscillation has been shown to be equal to the size of an external spanning vector of the bulk spacer Fermi surface. The oscillation amplitudes also depend on the curvature of the Fermi surface at the endpoints of these vectors. Finally, in the case of random binary alloy spacers an extra exponential damping term is present with a characteristic length which is related to the coherence lengths of the quasiparticle states at the endpoints of the external vector.[7,10,14]

Despite being disordered, the random binary alloys still have a periodic underlying lattice over which the two metallic-element atoms are randomly distributed and thus the *k*-space representation as well as the concept of Fermi surface are still useful.[15] A discussion of these ideas in terms of the Bloch spectral function (BSF) can be found in Refs. 8, 15 and 16 and will be briefly summarized here. By definition, the BSF is the number of states per energy and Bloch wave vector *k*. For constant energy and equal to the Fermi energy, it has peaks in *k*-space directions and these peaks mark the position of the Fermi surface. The fundamental difference between pure metals and random binary alloys is that these peaks are δ functions in the case of pure metals while in the case of random binary alloys, in the limit of small disorder, they are Lorentzian with finite height and width. The Fermi surface is defined for the system if the width of the peaks is small compared to the size of geometrical features, such as necks or pockets, of the Fermi surface. Compared to pure metal case, the difference is the width of the peaks, which is also a function of the Bloch wave vector, and is related to the coherence length of the quasiparticle states. Interestingly, the characteristic length of the extra exponential factor in the energy of the OEC across alloy spacers as a function of thickness is also related to the widths of the BSF at the end points of the extremal vectors.[7,8]

For metallic materials with finite quasiparticles coherence lengths, such as the random binary alloys, the well established, powerful and frequently exploited technique of the De Haas–van Alphen oscillations[17,18] (dHvA) is not applicable since the electrons cannot complete closed paths in *k* space without being scattered. Thus, the OEC phenomenon which is clearly observable and is closely related to the spacer Fermi surface, could become a useful probe of the Fermi surface[8] competing with the only alternative experimental technique of two-dimensional (2D) angular correlation of positron annihilation radiation (ACAR).[19] Although it appears to be very difficult to reconstruct fully a complex Fermi surface, such as that of a transition metal, from OEC measurements, they readily yield useful quantitative information on the size of necks or pockets of the Fermi surface. Evidently, to get the most out of the OEC experiments, theoretical calculations of the OEC are required for interpretation. Clearly, these are most fruitful if, as in Ref. 10, the interaction energy is decomposed into contributions from specific extremal vectors of the Fermi surface of the spacer. In what follows, we deploy this very effective approach to the problem of an alloy spacer.

Experimental studies on the OEC across alloy spacers have been performed for $Co/Cu_{(1-x)}Ni_x/Co$ (Refs. 20–24) for the (111) and the (110) growth orientations. Large period oscillations, of the order of 10 Å, were found for both these orientations for all concentrations of Ni ($x<0.5$). These oscillations are believed to be generated by extremal vectors in

the area of the neck[4,6,7,23] of the Cu-like Fermi surface of these alloys. In the case of (110) orientation, the spanning vector is the diameter of the circular cross section of the neck of the Cu-like Fermi surface, while in the case of (111) orientation the oscillation is believed[7] to originate from the spanning vector at an angle of 19.47°. Thus, the sizes of the two periods are close to each other. However, the oscillation period for the (111) growth orientation is slightly smaller. There is remarkable agreement between the periods of the OEC across these alloys[23,24] and the Korringa-Kohn-Rostoker (KKR) coherence potential approximation (CPA) calculations[7,8] of the Fermi surface of these alloys. In addition to the periods, the experimentally observed lack of damping in these oscillations has been successfully related to the calculated small widths of the Lorentzian-like Bloch-spectral functions (BSF's) at the end points of the extremal vectors for all these alloy spacers.[7,8] However, the phases and the amplitudes will be treated here on the basis of the first-principles calculations. Of course, we can approach the problem from the point of view of total energy calculations, but they do not connect amplitudes and phases information directly to spanning vectors of the Fermi surfaces and hence, from the point of view of our present concerns, they are not as useful as the asymptotic approach. Such total energy calculations have been performed for the Co/$Cu_{(1-x)}M_x$/Co (100) system, with $M=$Ni, Zn, Au using the tight-binding (TB)–linearized-muffin-tin-orbital (LMTO) electronic structure method and the coherence potential approximation.[25–27] These calculations serve as a reference to compare our results with, and we will refer to them later in this work.

In short, in the present work, we present the first application of our theoretical approach introduced in Ref. 10 to the case of $Cu_{(1-x)}Ni_x$ alloy spacers. More specifically, we compare the results obtained with the use of the asymptotic analysis to those obtained with full calculation of the OEC energy as well as the experiment. In addition we illustrate how structural changes of the Fermi surface, also referred as electronic topological transitions[16] (ETT's) could be probed using the OEC. Finally, we present conclusive evidence for the effect of the exponential decay of the oscillations for substitutionaly disordered spacers. In Sec. II we present briefly the formalism on which we based our calculations. The results of such calculations are discussed in Sec. III.

II. THE ASYMPTOTIC APPROACH

In this section we present the main points of the theoretical approach we used in our calculations. The details of this approach have already been published elsewhere[10,14] and is based on the screened Korringa-Kohn-Rostoker[28] and the KKR-CPA (Ref. 15) electronic structure methods.

The problem at hand is the magnetic interaction of two ferromagnetic layers which will be considered to be semi-infinite in our treatment, separated by a nonmagnetic but still metallic spacer layer. The spacer layer is substitutionaly disordered, i.e., a random, binary alloy. A uniform lattice is assumed for the entire system, namely we do not consider any lattice mismatch in the interfaces. Furthermore, these interfaces are regarded perfect, i.e., no surface roughness is present. From now on we will use the letters L and R for the left and right ferromagnetic layers and C for the finite spacer layer. In Ref. 10 we followed ideas presented in Refs. 29 and 30, but we employed the screened KKR formalism[28] and a layer by layer representation, and we wrote the interaction part of the grand potential in the form

$$\Delta\Omega_{LR}=\frac{1}{\pi}\int_{-\infty}^{\infty}dE f(E)\frac{S}{(2\pi)^2}\int_{(SBZ)}d^2\mathbf{k}_{\parallel}T(\mathbf{k}_{\parallel};E), \quad (1)$$

where $T(\mathbf{k}_{\parallel};E)\equiv\mathrm{Im}\{\mathrm{Tr}\{\hat{\Delta}_L[\tau_{CC}]_{1,N}\hat{\Delta}_R[\tau_{CC}]_{N,1}\}\}$ with $\hat{\Delta}_L=\Delta_L(1-\tau_{CC}\Delta_L)^{-1}$, $\hat{\Delta}_R=\Delta_R(1-\tau_{CC}\Delta_R)^{-1}$. Finally, $\Delta_L=G_{CL}\tau_{LL}G_{LC}$, $\Delta_R=G_{CR}\tau_{RR}G_{RC}$. In the above formulas $f(E)$ is the Fermi-Dirac distribution function, S is the area per surface atom, and the $\mathbf{k}_{\parallel}$ integration is taken over the first surface Brillouin zone. The L, C, and R indices refer to the three layers of the structure. The quantities $\tau_{LL}=M_{LL}^{-1}$, $\tau_{CC}=M_{CC}^{-1}$, $\tau_{RR}=M_{RR}^{-1}$ are the inverse KKR matrices, with τ_{CC} being finite in the perpendicular direction, while the other two being semi-infinite. Finally, N is the number of monolayers in the spacer and the quantities G_{CL}, G_{LC}, G_{CR}, and G_{RC} are the screened structure constant matrices. The disorder is introduced in the spacer slab through an effective one-site scattering matrix

$$M_{CC}=[t^{\mathrm{eff}}]^{-1}-G_{CC}, \quad (2)$$

with t^{eff} being the effective t-matrix calculated with the CPA. Clearly, due to screening, $\hat{\Delta}_L$ and $\hat{\Delta}_R$ are properties of the interfaces only.

In the light of arguments advanced in Ref. 10 [see discussion of Eq. (11) in Ref. 10] whatever is the method of calculation of T, and the technique for carrying the energy integral in Eq. (1), we are left with an expression for $\Delta\Omega_{LR}$ which for large spacer thickness D can be approximated by

$$\Delta\Omega_{\mathrm{LR}}=\mathrm{Im}\left\{\int_{(SBZ)}d^2\mathbf{k}_{\parallel}F(\mathbf{k}_{\parallel})\right\}$$
$$\simeq\mathrm{Im}\left\{\int_{(SBZ)}d^2\mathbf{k}_{\parallel}\sum_{\nu\nu'}g_{\nu\nu'}(\mathbf{k}_{\parallel})e^{iQ_{\nu\nu'}D}\right\}\frac{1}{D}. \quad (3)$$

In other words it is assumed that the integrand $F(\mathbf{k}_{\parallel})$ consists of simple exponential contributions. The sum is over pairs of branches ν, ν' of the Fermi surface of the spacer. The exponents are assumed to be linear in the spacer thickness D and that is referred as the linear phase approximation in Ref. 10. It is exact in the asymptotic limit $D\to\infty$. In the same asymptotic limit $g_{\nu\nu'}(\mathbf{k}_{\parallel})$ is independent of D. This can be easily seen from the asymptotic form of the energy integral[10] in Eq. (1). The quantities $Q_{\nu\nu'}$ are complex in the case of alloy spacers $Q_{\nu\nu'}=Q_{\nu\nu'}^{(R)}+iQ_{\nu\nu'}^{(I)}$. In the limit of small disorder, which is the case of interest in this paper, their real part $Q_{\nu\nu'}^{(R)}$ is the spanning vector of the Fermi surface parallel to the growth direction that connects the ν and ν' sheets of the Fermi surface. That spanning vector is of course a function of $\mathbf{k}_{\parallel}$. The imaginary part $Q_{\nu\nu'}^{(I)}$ is the sum of the half-widths of the Lorentzian-like BSF at the end points of the spanning vector, as it is shown in Ref. 10.

The particular form of the Eq. (3) makes it possible to use asymptotic analysis in the evaluation of the integrals for large spacer thicknesses.[31] In the limit of small disorder the

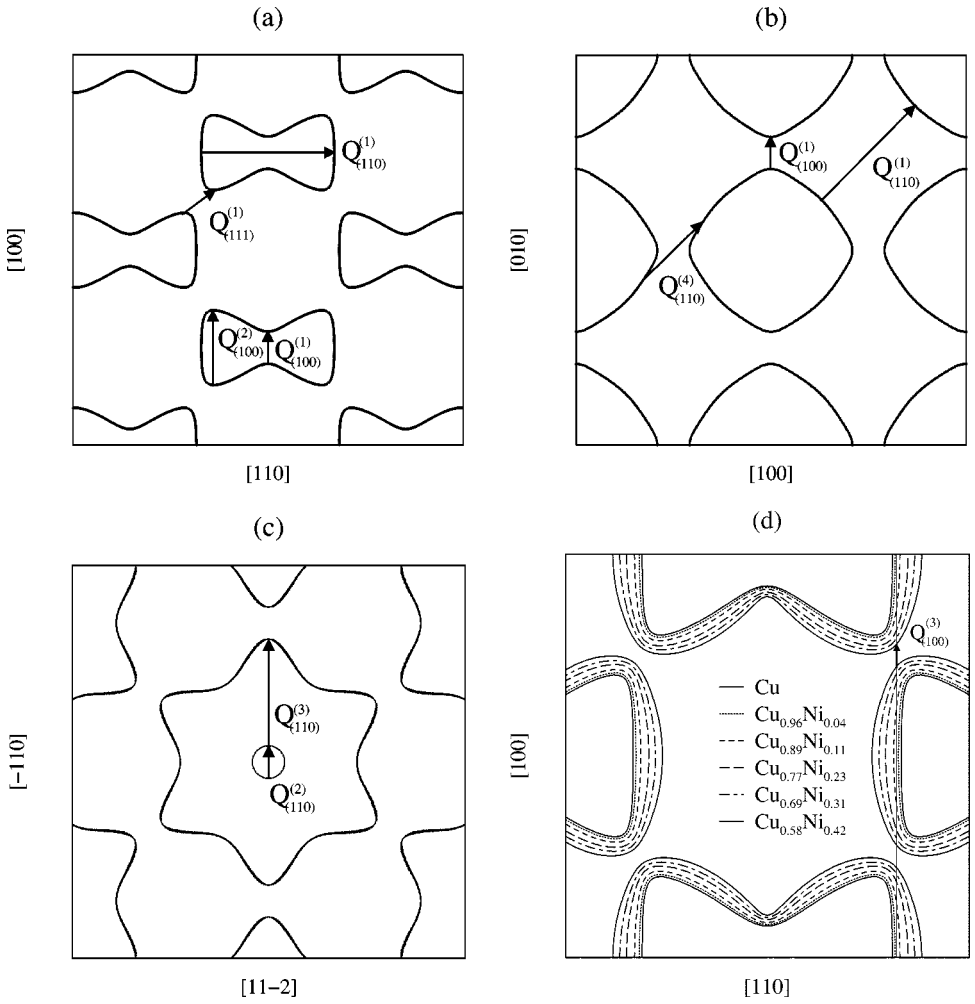

FIG. 1. The extremal vectors of Cu Fermi surface on three intersections plotted in the repeated zone scheme: an intersection perpendicular to the [1–10] direction at a distance $\Delta k=0$ to the Γ point (a), perpendicular to the [001], $\Delta k=0$ (b), and perpendicular to the [111], $\Delta k=\sqrt{3}/2$ (c). The evolution of the Fermi surface with Ni concentration is illustrated in (d). The $Q^{(3)}_{(100)}$ extremal vector which emerges as we increase Ni concentration is also shown in (d).

asymptotic analysis method will involve the stationary points of the real part of $Q_{\nu\nu'}(\mathbf{k}_\parallel)$. Indeed, a first approximation is to assume that $Q^{(I)}_{\nu\nu'}(\mathbf{k}_\parallel)$ is constant in the region that the $Q^{(R)}_{\nu\nu'}$ is stationary, since $Q^{(I)}_{\nu\nu'}$ is very small compared to $Q^{(R)}_{\nu\nu'}$ and on the other hand it is a smooth function of $\mathbf{k}_\parallel$. Under these circumstances the case is similar to that of pure metal spacers and the final result is

$$\Delta\Omega_{LR}(D)\simeq\frac{1}{D}\sum_{\mu}\ \mathrm{Im}\{A_\mu e^{iQ^{(\mu)}D}\},\tag{4}$$

with

$$A_\mu(D)=2\pi g_\mu\zeta(\xi_1^{(\mu)},D)\zeta(\xi_2^{(\mu)},D)\tag{5}$$

and

$$\zeta(\xi,D)=\begin{cases}\dfrac{1}{\sqrt{D}}\dfrac{e^{i(\pi/4)(\xi/|\xi|)}}{\sqrt{|\xi|}} & \text{for } \xi\neq 0,\\ \text{const} & \text{for } \xi=0.\end{cases}\tag{6}$$

In the above expressions the index μ counts the extremal vectors of the Fermi surface for the particular orientation, i.e., these $\mathbf{k}_\parallel^{(\mu)}$ points at which $Q^{(R)}_{\nu\nu'}(\mathbf{k}_\parallel)$ is extremal for any pair of indices ν, ν' and $Q^{(\mu)}=Q_{\nu\nu'}(\mathbf{k}_\parallel^{(\mu)})$, $g_\mu=g_{\nu\nu'}(\mathbf{k}_\parallel^{(\mu)})$. Moreover, $\xi_1^{(\mu)}$, $\xi_2^{(\mu)}$ are the eigenvalues of the second derivative matrix of $Q^{(R)}_{\nu\nu'}(\mathbf{k}_\parallel)$ at the extremal point $\mathbf{k}_\parallel^{(\mu)}$. We notice that $\Delta\Omega_{LR}$ depends on D as D^{-2} in the most common case in which both the eigenvalues, $\xi_1^{(\mu)}$ and $\xi_2^{(\mu)}$, are nonzero, as $D^{-3/2}$ if only one eigenvalue is nonzero, and as D^{-1} if both $\xi_1^{(\mu)}$ and $\xi_2^{(\mu)}$ are zero. The last two cases correspond to the partial and the complete nesting of the Fermi surface, according to the classification of Ref. 32. Finally, we would like to note that the real part of the $Q^{(\mu)}$, i.e., the wave vector of each of the oscillations, is the size of the extremal spanning vector of the real Fermi surface. Interestingly, the small imaginary part of $Q^{(\mu)}$, i.e., the inverse characteristic length of the exponential decay, is the sum of the half-widths of the Lorentzian-like peaks at the end points of that extremal vector. The inverse of each of these half-widths is the coherence length of the quasiparticle states at that point of the Fermi surface, as it is well explained in Refs. 7 and 8.

We will finish this brief review of the formal results that we shall make use of, by giving a few details concerning the actual calculation. The scalar relativistic KKR was used and the quantity we calculated is the energy difference

$$\delta\Omega_{LR}=\Delta\Omega_{LR}^{FM}-\Delta\Omega_{LR}^{AF},\tag{7}$$

where $\Delta\Omega_{LR}^{FM}$ is the OEC energy, given by Eq. (4), for the ferromagnetic (FM) orientation of the magnetic moments of L and R layers and $\Delta\Omega_{LR}^{AF}$ is the OEC energy for the antiferromagnetic (AF). The principal layers formulation was em-

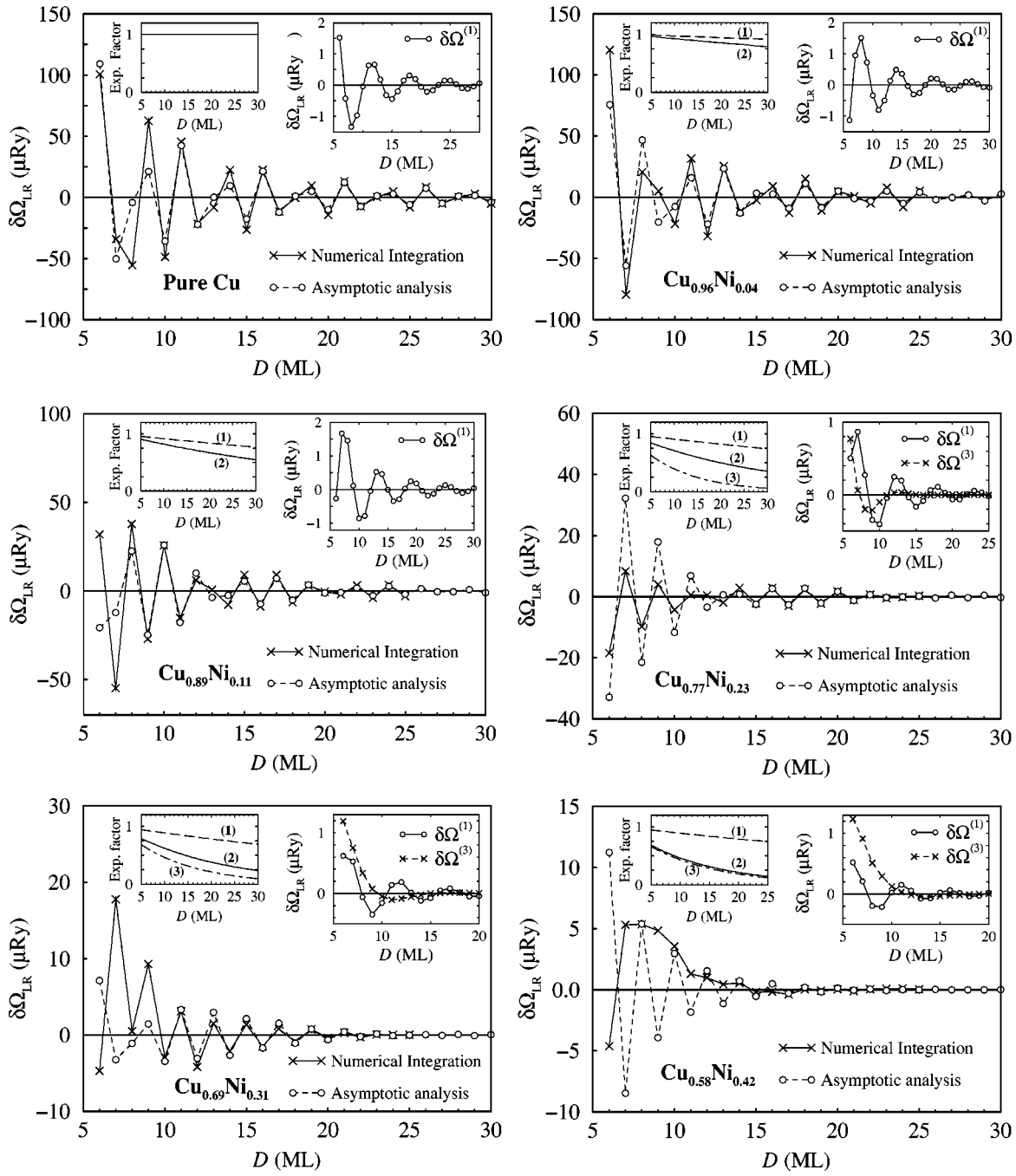

FIG. 2. The calculated energy difference (per surface atom) between the FM and AF configurations for the Co/$Cu_{(1-x)}Ni_x$/Co in the (100) orientation for the indicated Ni concentrations as a function of spacer thickness D. The full integration energy is plotted together with the asymptotic result which is dominated by the contribution from the $Q^{(2)}_{(100)}$ extremal vector. In the insets on the right of each plot we show $\delta\Omega^{(1)}$ and $\delta\Omega^{(3)}$, i.e., the contributions from $Q^{(1)}_{(100)}$ and $Q^{(3)}_{(100)}$ extremal vectors. In the insets on the left we have included the exponential decay factor as a function of spacer thickness.

ployed, thus within the screened KKR method the range of structure constant was restricted to the next nearest principal-layer only. A principal layer was assumed to consist of three atomic layers. The calculation of $\hat{\Delta}_L, \hat{\Delta}_R$ requires the calculation of τ_{LL} and τ_{RR} which in the case of screened KKR can be done for the required semi-infinite geometry by using iterative techniques.[28] By contrast, the calculation of τ_{CC} for the spacer slab is a straightforward inversion of M_{CC}, since the matrix has finite dimension. To facilitate the calculation we used an analog of the Eq. (4) involving quantities directly available from calculation with the layered KKR code. Thus, we used the integrand function F in Eq. (3), calculated at the loci of the extremal vectors, as we explain in Ref. 10. Finally, as we have already mentioned, the integrations over E has been carried out numerically using the Matsubara poles technique for finite temperature $T=300\,\mathrm{K}$ and in our case 5–10 poles were found to be enough to achieve convergence. The ASA approximation was used in the KKR method and the maximum angular momentum quantum number $l_{\max}$ was taken $l_{\max}=2$. As we will see in the next section, this is a

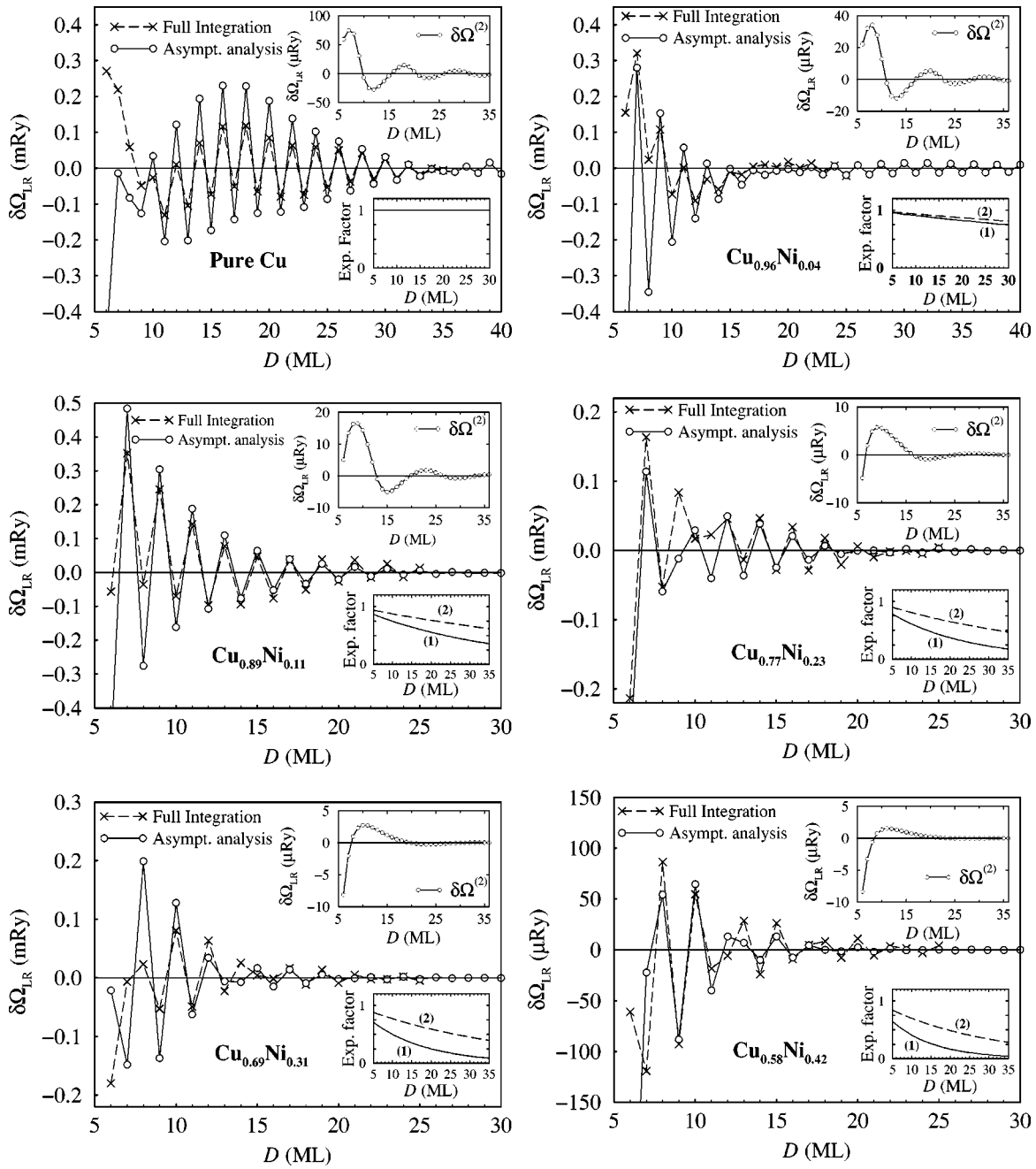

FIG. 3. The calculated energy difference (per surface atom) between the FM and AF configurations for the $Co/Cu_{(1-x)}Ni_x/Co$ in the (110) orientation for the indicated concentrations as a function of spacer thickness D. The full integration is compared with the asymptotic result dominated by the contribution from the $Q^{(1)}_{(110)}$ extremal vector. The contribution from the $Q^{(2)}_{(110)}$ extremal vector ($\delta\Omega^{(2)}$) is plotted in the insets on the top right, while the exponential decay factors for the two contributions are plotted in the insets on the bottom right.

limitation of the current state of the code we use. However, the consequences of this do not affect the conclusions of the present work. Finally, the lattice parameter for the alloys was assumed to scale linearly with concentration (Vegard's law).

III. RESULTS

In our calculations we considered $Co/Cu_{(1-x)}Ni_x/Co$ spacers with concentrations $x=0.04$, 0.11, 0.23, 0.31, and 0.42. We calculated the OEC for all the (100), (110), and (111) orientations. The integration over $k_\parallel$ was carried out both by full numerical integration and by using the saddle-point asymptotic method described in Sec. II. Our results should be viewed in conjunction with these of Ref. 10 for pure Cu. Nevertheless, some of these results are also shown here for completeness. It is well known that the Fermi surface of the bulk $Cu_{(1-x)}Ni_x$ does not undergo dramatic structural changes with increasing x (for $x \leqslant 0.42$). Hence it is rather similar to that of pure Cu. Consequently, the extremal vectors for the alloy Fermi surfaces originate from the equivalent points of the pure Cu Fermi surface and change only in size. Thus we find it useful to include Fig. 1 showing all the Cu-Fermi-surface extremal vectors for reference. Additionally we have depicted the evolution of the Fermi surface with alloying in Fig. 1(d). Interestingly, the above remarks not withstanding, there is an extremal vector for the

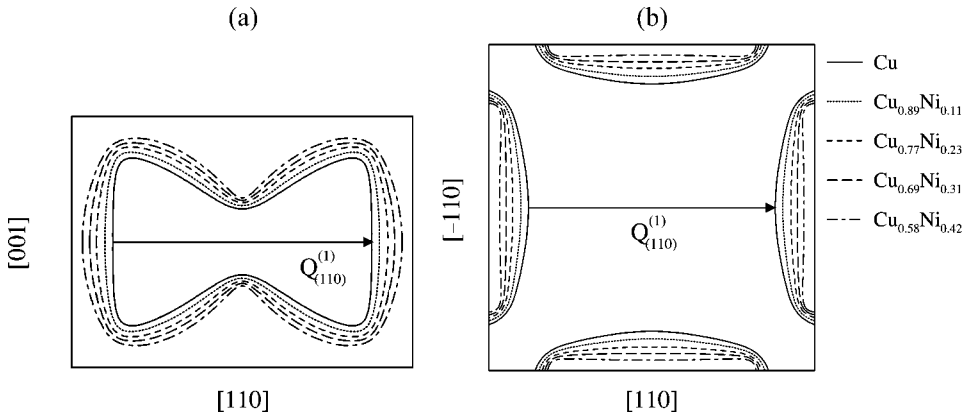

FIG. 4. The $Q^{(1)}_{(110)}$ extremal vector on two perpendicular intersections of the Fermi surface: (a) perpendicular to the $[-110]$ and (b) perpendicular to the [001] both through the Γ point. In (a) the Fermi surface around the extremal vector is flat for pure Cu and is curved as Ni concentration increases. In (b) the Fermi surface flattens as Ni is added and it becomes absolutely flat at some concentration close to $x=0.31$.

(100) orientation, namely the $Q^{(3)}_{(100)}$, which is not present for pure Cu or small Ni concentrations. This is included in Fig. 1(d) and will be the subject of comments later in this paper. In interest of clarity the following subsections record our findings for the three growth orientations separately.

A. The (100) orientation

As shown in Fig. 1 there are three extremal vectors for the (100) orientation. The $Q^{(1)}_{(100)}$ and $Q^{(2)}_{(100)}$ were also present in the case of pure Cu,[10] while the third one $Q^{(3)}_{(100)}$ is a result of the Fermi surface change with alloying, as shown in Fig. 1(d). In Fig. 2 we show our results for the OEC energy for all the concentrations we considered. As can be seen, there is a very good agreement between the full integration result and the asymptotic analysis. Our result is strong evidence for the validity of the generalized asymptotic analysis approach introduced in Ref. 10. Particularly noteworthy is the fact that the exponential decay with the spacer thickness predicted by the asymptotic analysis is verified by the full calculations. Indeed, the exponential term in the asymptotic result given in the Eq. (4), is a consequence of $Q^{(m)}$ having an imaginary part in the case of disordered spacer. The strength of that term is shown in the insets of Fig. 2. Apparently, the inclusion of this factor is crucial in achieving the remarkable agreement between the asymptotic analysis and the full integration results.

For the $Co/Cu_{(1-x)}Ni_x/Co(100)$ system there are available total energy calculations[25,26] for $x=0$, 0.10 (Ref. 25) and 0.25,[26] as mentioned earlier. These calculations were performed using the TB-LMTO electronic structure method treating the alloy spacer in terms of the CPA. In Ref. 26, the CPA is compared with the virtual crystal approximation, and it is proven that for the $Co/Cu_{(1-x)}Ni_x/Co(100)$ system the more accurate treatment in terms of the CPA is required. It is pleasing to note that our calculations agree remarkably well with the results of Refs. 25 and 26 concerning both the amplitudes and the periods and phases of the oscillations for both pure Cu and for $x>0$. Although the concentrations considered in Refs. 25 and 26, i.e., $x=0.1$ and 0.25 were not considered in our study, one could compare these results with our results for $x=0.11$ and $x=0.23$. Given the small concentration difference, there is a very good quantitative agreement in all the coupling characteristics.

As in the case of pure Cu spacer,[10] the small-period oscillation of approximately 2 ML, corresponding to $Q^{(2)}_{(100)}$, is the dominant. It is pleasing to note that a dramatic phase change with alloying is well reproduced by the asymptotic analysis. Although the amplitude gradually decreases with Ni concentration, the oscillatory behavior is preserved even for 31% Ni. For the largest Ni concentration (42%) there is no oscillatory behavior present in the full calculation result. Nevertheless, even for that concentration the order of magnitude of the OEC energy is still the same for the two calculations. A word of caution is in order concerning the small disorder assumption in the asymptotic analysis for the large Ni concentrations. The ratio of amplitudes $A^{(2)}_{(100)}/A^{(1)}_{(100)}$ of the oscillation terms corresponding to $Q^{(2)}_{(100)}$ and $Q^{(1)}_{(100)}$ decreases significantly with x from $\sim 65-70$ for small concentrations to $\sim 10-20$ for large.

As we have already mentioned a new extremal vector, $Q^{(3)}_{(100)}$ in Fig. 1(d), appears for relatively large concentrations

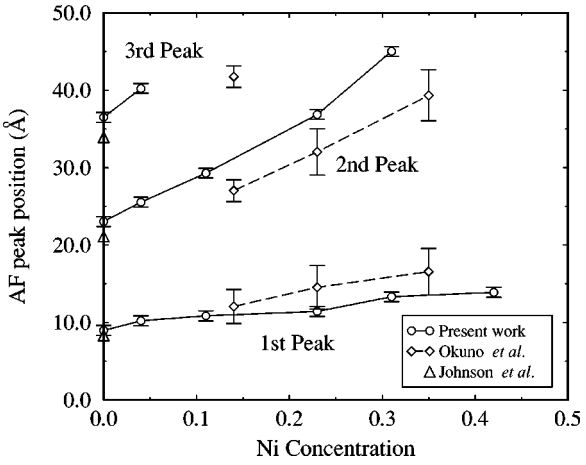

FIG. 5. Comparison of the calculated position of the AF peaks for the (110) orientation with the experiments of Okuno and Inomata (Refs. 23 and 24) and Johnson *et al.* (Ref. 38). The experimental error bars in the experimental results are deduced from the pictures of GMR versus spacer thickness of Refs. 23 and 24.

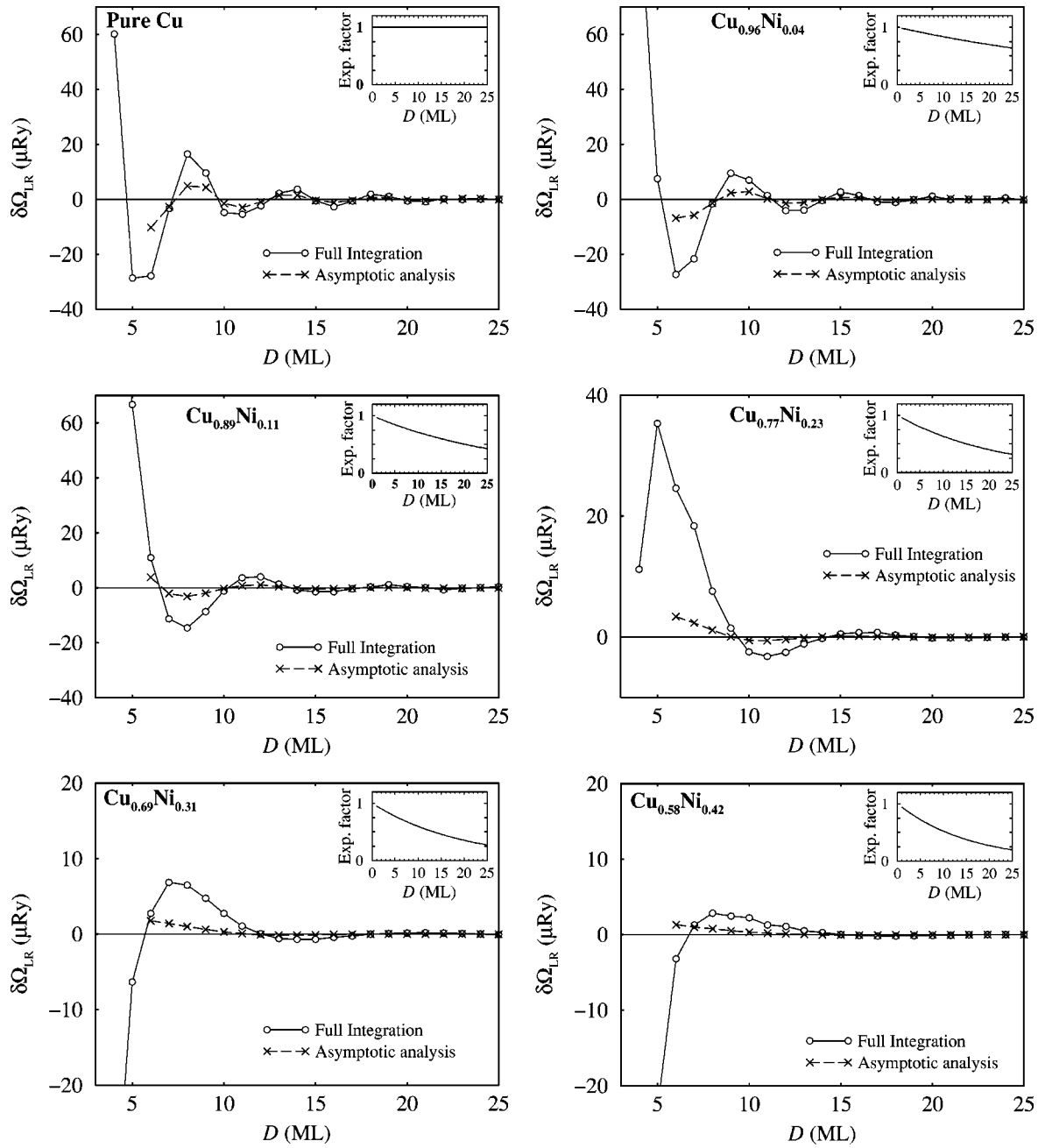

FIG. 6. The calculated energy difference (per surface atom) between the FM and AF configurations for the Co/$Cu_{(1-x)}Ni_x$/Co in the (111) orientation for the indicated concentrations as a function of spacer thickness D: comparison of the full integration with the asymptotic analysis result. The exponential decay factor is shown in the insets.

of Ni. It is the result of the progressive increase with x of the holelike ''dog bone'' of the Fermi surface as can be seen in Fig. 1(d), and the relevant period increases rapidly with x. The size of that period is 4.00, 7.30, 10.42, 18.2 ML for the Ni concentrations $x=0.11$, 0.23, 0.31, and 0.42, respectively. The emergence of this extremal vector can be considered as a precursor of the ETT that occurs for larger Ni concentration than these considered in this work and which consists of the complete vanishing of the neck. Unfortunately, we could not deal with these interesting cases in the present work because, in such study, one should consider magnetism in the spacer layer as well as in the magnetic layers. Although the contribution to the OEC corresponding to $Q^{(3)}_{(100)}$ is small compared to that corresponding to $Q^{(2)}_{(100)}$ by at least an order of magnitude, it is larger than that corresponding to $Q^{(1)}_{(100)}$ for large concentrations. This is shown in the insets of Fig. 2. Obviously, it would be interesting to detect the emergence of this topological feature, but, to our knowledge, there are no OEC experiments concerning the (100) growth orientation for the Co/$Cu_{(1-x)}Ni_x$/Co system for $x\neq 0$. Moreover, we reckon that it is difficult for current OEC experiments to detect the emergence of $Q^{(3)}_{(100)}$ for two reasons: first the OEC is dominated by the oscillation corresponding to $Q^{(2)}_{(100)}$. Nevertheless, the period of that oscillation is very small and, more often than not, these small period oscillations are suppressed by interface roughness.[33] Secondly, it is not easy to distinguish experimentally between the contribution corresponding to $Q^{(3)}_{(100)}$ and $Q^{(1)}_{(100)}$. In any case, we highlighted

this feature to call attention to the fact that such phenomena can occur and may play a more significant role in the case of other transition metal alloy spacers.

B. The (110) orientation

As can be seen in Fig. 1 there are four different extremal vectors for the (110) orientation. For pure Cu,[10] only two of them, namely, the $Q^{(1)}_{(110)}$ and $Q^{(2)}_{(110)}$, were found to have significant contribution and they are the only ones we have considered for the $Cu_{(1-x)}Ni_x$ spacers as well. In Fig. 3 we again show the full numerical result together with the asymptotic one for all the concentrations we examined. As in the pure Cu case,[10] the small-period oscillation corresponding to the $Q^{(1)}_{(110)}$ extremal vector in Fig. 1(a) is dominating the OEC. More specifically, the ratio of the amplitudes of the two contributions is of the order of 5–10 for pure Cu and small Ni concentration, but it rapidly increases to the order of 100–200 for large Ni concentration. The small period oscillation appears to be the strongest of all contributions for all three orientations considered. We should mention here that $Q^{(1)}_{(110)}$ is the vector spanning the belly of the Fermi surface along the (110) orientation and it is the same vector that drives the ordering process and the concentration waves in Cu-Pd alloys.[34,35]

The size of the OEC energy $\delta\Omega_{LR}$ corresponding to the dominant contribution changes much less with alloying than that of the contribution corresponding to the $Q^{(2)}_{(110)}$, despite the fact that the exponential damping for the dominant oscillation is stronger, as shown in the insets of Fig. 3. Interestingly, the related amplitude, $A^{(1)}_{(110)}$, does not change monotonically, but has two maximum values at Ni concentrations $x=0$ and $x=0.31$. This effect has Fermi surface geometrical origin and it is the result of the flattening of the Fermi surface at the neighborhood of the endpoints of $Q^{(1)}_{(110)}$. That can be seen in Fig. 4(b) where the increase of Ni concentration results in Fermi surface flattening along the $[-110]$ perpendicular to the spanning vector orientation. Unfortunately, that flattening is compensated by the curving of the Fermi surface along the [001] direction as seen in Fig. 4(a). In other words, while one of the two eigenvalues of the second derivative matrix of the extremal vector $\xi_{[001]}$ is minimal at $x=0$, the other one $\xi_{[-110]}$ is minimal at some concentration close to 0.31. Unfortunately, another contributing factor, namely the aliasing effect, affects dramatically the OEC and as a result the strongest calculated oscillation appears at $x=0.11$, among the concentrations we considered, as seen in Fig. 3. Of course, in order to find the exact Ni concentration at which the calculated OEC is maximum, the consideration of many different concentrations is required.

Again for the (110) orientation, the asymptotic analysis reproduces the coupling behavior including the exponential decay term for the whole range of concentrations, despite the fact that the Fermi surface is very flat in the neighborhood of $Q^{(1)}_{(110)}$ extremal vector. Contrary to the (100) orientation, there is oscillatory behavior of the coupling for largest Ni concentration (42%) for the full integration result as well.

For the (110) orientation there are experimental data from Okuno and Inomata[23,24] on the GMR ratio versus the spacer thickness for the $Co/Cu_{(1-x)}Ni_x/Co$ system for three different Ni concentrations ($x<0.5$). Since only one large period oscillation appears in the experiment of Okuno and Inomata, we can compare our asymptotic-analysis AF peaks for the contribution corresponding to the $Q^{(2)}_{(110)}$ to those experimental peaks. That comparison is shown in Fig. 5. Our calculated AF peak positions are in general close to the experimental ones. In addition, the general trend of the peaks moving to higher thicknesses for higher concentrations is reproduced by our results. Nevertheless, it seems that the oscillation periods are not in such a good agreement with the experimental ones of Okuno and Inomata as the ones calculated using KKR-CPA, with $l_{\max}=3$, published in Ref. 7. That fact can be seen in Fig. 5 where although the first peak is in good agreement with the experiment the second and third are not, and they are moved to higher thicknesses compared with the experimental. Obviously, it is the case that small periods are predicted more accurately from the Fermi surface analysis than the large ones, such as the one considered here, since they correspond to large extremal vectors. What a bulk Fermi surface calculation shows is that the present KKR scheme with $l_{\max}=2$ underestimates slightly the size of the already very small neck of the Fermi surface for the whole range of Ni concentrations considered. That is reflected in the OEC calculation by the small deviations of the position of the AF peaks. This conclusion is also supported by the very good agreement of the calculated oscillation periods of Ref. 7 where $l_{\max}=3$ was used with the ones from the Okuno and Inomata experiments.[23,24]

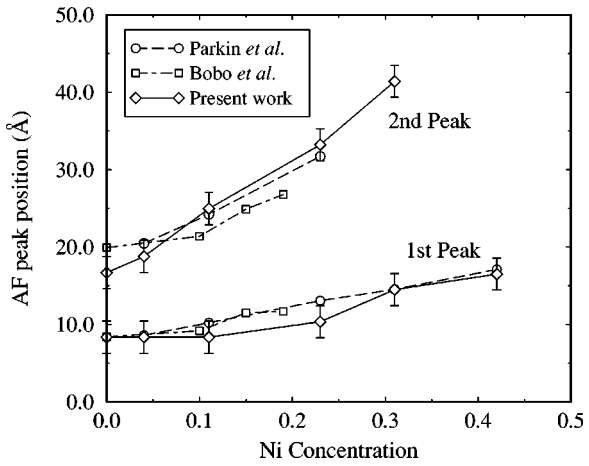

FIG. 7. Comparison of the calculated position of the AF peaks for the (111) orientation with the experiments of Parkin *et al.* (Ref. 22) and Bobo *et al.* (Ref. 21).

The absence of the small period in experiments, although is is found to dominate the OEC for both pure Cu (Refs. 10 and 33) and Cu-Ni alloy spacers, is believed to be a consequence of the surface roughness.[33] Nevertheless, in other cases, such as Co/Cu/Co (100) (Ref. 36) or Fe/Cr/Fe (100),[37] small periodicities in the OEC have been detected. It would be interesting to see whether the effect of the nonmonotonic behavior with x of the strength of the short period oscillation could be experimentally detected for the $Co/Cu_{(1-x)}Ni_x/Co(110)$.

C. The (111) orientation

Again, in Fig. 6, we show the results of both the full numerical and the asymptotic analysis for the (111) orienta-

tion. Systematically, the full numerical result is a factor of 2 larger than the asymptotic result, as in the case of pure Cu.[10] Nevertheless, the period, the amplitude and the phase are in very good agreement with experiment for pure Cu,[10] while the dependence of the period on the Ni concentration also follows closely the experimental data.[7] Our calculations, despite the limitation ($l_{\max}=2$) considered above, succeeds to reproduce the position of the AF peaks for the (111) direction as it is shown in Fig. 7, where we have plotted the first and second calculated AF-peak positions as functions of Ni concentration as well as the experimental positions[21,22] for comparison. Both these experiments as well as the experiments of Okuno and Inomata[23,24] mentioned above are measurements of the GMR ratio as function of spacer thickness. Thus we do not have the chance to compare the calculated amplitudes with the experiment. Nevertheless, in the case of pure Cu,[10] these amplitudes were found in very good agreement with experiment, given the fact that this kind of comparison is usually restricted to the order of magnitude.

IV. CONCLUSION

In summary, we calculated the oscillatory exchange coupling (OEC) for the Co/$Cu_{(1-x)}Ni_x$/Co trilayer system for all the (100), (110), and (111) orientation, using first-principles asymptotics and compared the results with the full calculation. The good agreement between these two approaches demonstrate the correctness and the power of the asymptotic analysis in the context of a first-principles, screened, KKR-CPA method for random alloys as well as for pure metal spacers. In particular, we have discovered the emergence of an additional extremal spanning vector of the Fermi surface of Co/$Cu_{(1-x)}Ni_x$/Co for the (100) orientation [$Q^{(3)}_{100}$ in Fig. 1(d)]. While this is an interesting change in the Fermi surface we believe it is not clear if it could be observed by the currently employed experiments. Hopefully, in the case of other transition metal alloys, similar Fermi surface changes may play a more significant role in the OEC. Thus, we conclude by pointing out that measurements of the OEC is a good way for searching for the elusive electronic topological transitions[16] in addition to being a powerful general probe of the alloy Fermi surfaces.

ACKNOWLEDGMENTS

One of the authors (N.N.L.) had financial support by the TMR network on ''Interface Magnetism'' (Contract No. ERBFMRXCT960089) of the European Union and PAIS ELMAMES of the INFM (Italy).

[1] M. N. Baibich, J. M. Broto, A. Fert, F. Nguyen Van Dau, F. Petroff, P. Etienne, G. Creuzet, A. Friederich, and J. Chazelas, Phys. Rev. Lett. **61**, 2472 (1988).
[2] G. Binasch, P. Grunberg, F. Saurenbach, and W. Zinn, Phys. Rev. B **39**, 4828 (1989).
[3] S. S. P. Parkin, N. More, and K. P. Roche, Phys. Rev. Lett. **64**, 2304 (1990).
[4] P. Bruno and C. Chappert, Phys. Rev. Lett. **67**, 1602 (1991).
[5] P. Bruno and C. Chappert, Phys. Rev. B **46**, 261 (1992).
[6] *Ultrathin Magnetic Structures II*, edited by B. Heinrich and J. A. C. Bland (Springer-Verlag, Berlin, 1994).
[7] N. N. Lathiotakis, B. L. Györffy, B. Újfalussy, and J. Staunton, J. Magn. Magn. Mater. **185**, 293 (1998).
[8] N. N. Lathiotakis, B. L. Györffy, and J. B. Staunton, J. Phys.: Condens. Matter **10**, 10 357 (1998).
[9] N. N. Lathiotakis, B. L. Györffy, E. Bruno, B. Ginatempo, and S. S. P. Parkin, Phys. Rev. Lett. **83**, 215 (1999).
[10] N. N. Lathiotakis, B. L. Györffy, and B. Újfalussy, Phys. Rev. B **61**, 6854 (2000).
[11] D. D. Koelling, Phys. Rev. B **59**, 6351 (1999).
[12] C.-Y. You, C. H. Sowers, A. Inomata, J. S. Jiang, S. D. Bader, and D. D. Koelling, J. Appl. Phys. **85**, 5889 (1999).
[13] M. D. Stiles, J. Magn. Magn. Mater. **200**, 322 (1999).
[14] B. Újfalussy, N. N. Lathiotakis, B. L. Györffy, and J. B. Staunton, Philos. Mag. B **78**, 577 (1998).
[15] B. L. Györffy and G. M. Stocks, in *Electrons in Disordered Metals and at Metallic Surfaces*, Vol. 42 of *NATO Advanced Study Institute, Series B: Physics*, edited by P. Phariseau, B. L. Györffy, and L. Scheire (Plenum, New York, 1979), pp. 89–192.
[16] E. Bruno, B. Ginatempo, E. S. Giuliano, A. V. Ruban, and Y. Vekilov, Phys. Rep. **249**, 353 (1994).
[17] A. P. Cracknell and K. C. Wong, *The Fermi Surface* (Clarendon, Oxford, 1973).
[18] M. Springford, in *Electrons at the Fermi Surface*, edited by M. Springford (Cambridge University Press, Cambridge, 1980).
[19] S. Berko, in *Electrons in Disordered Metals and at Metallic Surfaces* (Ref. 15), pp. 239–291.
[20] F.-J. Bobo, L. Hennet, M. Piecuch, and J. Hubsch, Europhys. Lett. **24**, 139 (1993).
[21] F.-J. Bobo, L. Hennet, M. Piecuch, and J. Hubsch, J. Phys.: Condens. Matter **6**, 2689 (1994).
[22] S. S. P. Parkin, C. Chappert, and F. Herman, Europhys. Lett. **24**, 71 (1993).
[23] S. N. Okuno and K. Inomata, Phys. Rev. Lett. **70**, 1711 (1993).
[24] S. N. Okuno and K. Inomata, J. Magn. Magn. Mater. **126**, 403 (1993).
[25] P. Bruno, J. Kudrnovský, V. Drchal, and I. Turek, Phys. Rev. Lett. **76**, 4254 (1996).
[26] J. Kudrnovský, V. Drchal, P. Bruno, I. Turek, and P. Weinberger, Phys. Rev. B **54**, R3738 (1996).
[27] I. Turek, V. Drchal, J. Kudrnovský, and M. Šob, *Electronic Structure of Disordered Alloys, Surfaces and Interfaces* (Kluwer, Dordecht, 1997).
[28] L. Szunyogh, B. Újfalussy, P. Weinberger, and J. Kollár, Phys. Rev. B **49**, 2721 (1994).
[29] E. Bruno and B. L. Györffy, J. Phys.: Condens. Matter **5**, 2109 (1993).
[30] E. Bruno, B. L. Györffy, and J. B. Staunton, in *Metallic Alloys: Experimental and Theoretical Perspectives*, Vol. 256 of *NATO Advanced Study Institute, Series E: Applied Sciences*, edited by J. S. Faulkner and R. G. Jordan (Kluwer Academic, Dordrecht, 1994), p. 321.
[31] C. M. Bender, and S. A. Orszag, *Advanced Mathematical Methods for Scientists and Engineers* (McGraw-Hill, New York, 1978).

[32] L. M. Roth, H. J. Zeiger, and T. A. Kaplan, Phys. Rev. **149**, 519 (1966).
[33] L. Nordstrom, P. Lang, R. Zeller, and P. H. Dederichs, Phys. Rev. B **50**, 13 058 (1994).
[34] B. L. Györffy and G. M. Stocks, Phys. Rev. Lett. **50**, 374 (1983).
[35] B. L. Györffy, D. D. Johnson, F. J. Pinski, D. M. Nicholson, and G. M. Stocks, in *Alloy Phase Stability*, Vol. 163 of *NATO Advanced Study Institute, Series E: Applied Sciences*, edited by G. M. Stocks and A. Gonis (Kluwer Academic, Amsterdam, 1989), pp. 421–468.
[36] M. T. Johnson, S. T. Purcell, N. W. E. McGee, R. Coehoorn, J. aan de Stegge, and W. Hoving, Phys. Rev. Lett. **68**, 2688 (1992).
[37] J. Unguris, R. J. Celotta, and D. T. Pierce, Phys. Rev. Lett. **67**, 140 (1991).
[38] M. T. Johnson, R. Coehoorn, J. J. de Vries, N. W. E. McGee, J. aan de Stegge, and P. J. H. Bloemen, Phys. Rev. Lett. **69**, 969 (1992).